Journal of Catalysis **202,** 367–378 (2001)
doi:10.1006/jcat.2001.3268, available online at http://www.idealibrary.com on IDEAL®

Effects of Pretreatments on the Surface Composition of Alumina-Supported Pd–Rh Catalysts

T. Maillet,* J. Barbier Jr.,* P. Gelin,† H. Praliaud,† and D. Duprez*,[1]

*Laboratoire de Catalyse en Chimie Organique, UMR 6503 CNRS/Université Poitiers, 40 Avenue Recteur Pineau, 86022 Poitiers Cedex, France; and †Laboratoire d'Application de la Chimie à l'Environnement, UMR 5634 CNRS/Université Claude Bernard Lyon l, 43 Bd. Du 11 Novembre 1918, 69622 Villeurbanne Cedex, France

Received March 5, 2001; accepted April 19, 2001; published online August 9, 2001

The surface composition of alumina-supported Pd, Rh, and Pd–Rh catalysts fresh or after high temperature treatments under oxidizing (O_2 in N_2) or reducing (H_2 in N_2) mixture has been characterized using various complementary techniques: chemisorption and titration of H_2 and O_2 probe molecules, $^{18}O_2/^{16}O_2$ isotopic equilibration (OIE), FTIR spectroscopy of adsorbed CO and NO, and electron microscopy with X analysis. From both techniques it is concluded that the surface composition is close to the bulk composition for all the fresh bimetallics, whatever the Rh content. The surface state of the bimetallics treated at 1173 K is strongly dependent on the nature of the gas mixture. There is a relative increase in surface Pd after treatment in an oxidative medium, because of a Rh^{3+} migration into alumina, and in surface Rh after treatment in a reducing medium. The specific role of alumina can explain these results, in contradiction with thermodynamic models predicting the reverse situation (enrichment in Rh in O_2 and in Pd in H_2). Activity for propane oxidation at 573 K and for propane steam reforming at 673 K was also determined over fresh and sintered catalysts. Because Pd is more active than Rh in oxidation and Rh is more active than Pd in steam reforming, activity changes with the Rh content, before and after sintering, may reflect modifications of surface composition. The results obtained with the series of Pd–Rh catalysts are in agreement with the measurements made by OIE and FTIR spectroscopy. The hypothesis and the conditions of applications of the methods are discussed.

Key Words: **palladium–rhodium bimetallic catalysts; $^{18}O_2$–$^{16}O_2$ isotopic equilibration; FTIR of CO and NO; surface composition of Pd–Rh; propane oxidation (over Pd–Rh catalysts); propane steam reforming (over Pd–Rh catalysts).**

1. INTRODUCTION

Bimetallic catalysts are widely used in automotive converters as three-way catalysts (TWC). Pt–Rh-based catalysts were developed first: they associated a very active metal for oxidation (Pt) to the most active and selective element for NOx reduction (Rh). More recently, more stringent standards were imposed by the European Community which also eliminated the 40-s pretest idle period. To meet these directives, new technologies with low light-off and thermally durable catalysts, set up very close to the engine, were developed. In this respect, Pd–Rh–Pt and Pd–Rh TWC were progressively introduced on the catalyst market (1–3). Palladium is more sensitive than platinum to poisons such as lead (4, 5) and sulfur (6, 7). Nevertheless, the introduction of unleaded, low-sulfur gasoline gave Pd a definitive advantage owing to its high thermal resistance, particularly in an oxidative medium (8). This made Pd-based catalysts good candidates for replacing the conventional Pt–Rh/CeO_2/Al_2O_3 catalysts (9, 10).

Activity and selectivity of bimetallic catalysts depend on several factors: (i) the degree of interaction between the two metals (e.g., separate phases and alloyed phases), (ii) the degree of interaction between the metals and the support, and (iii) the chemical state of the metals (more or less oxidized). All these factors can affect the surface composition, which is a key parameter in determining the performance of the bimetallic catalyst.

Contrary to Pt–Rh catalysts, relatively few studies were devoted to the characterization of Pd-based noble metal catalysts: Pd–Pt (11–15) and Pd–Rh (16–18). Under oxidizing conditions, it seemed that Pd–Pt and Pd–Rh alloys were enriched in palladium at $T <$ Td, temperature of PdO decomposition. However, palladium oxide and platinum particles would tend to segregate (11, 13) while rhodium could diffuse through the initial PdO upper layer without any phase separation of the alloy particles (16, 17). Contradictory results were obtained in methane oxidation over Pd–Rh catalysts: at 550°C, a detrimental interaction between the two metals was reported by Oh and Mitchell (19) while Ahlström-Silversand and Odenbrand concluded that the activity of Pd was promoted by Rh at 400°C (20). A similar synergy effect was observed by Araya and Diaz in CO oxidation over Rh–Pd/SiO_2 catalysts prepared by successive impregnation (21). Under reducing conditions, many Pd-based bimetallic solids would be enriched in

[1] To whom correspondence should be addressed. E-mail: Daniel.Duprez@univ-poitiers.fr.

0021-9517/01 $35.00

palladium over a wide temperature range (15, 22, 23). Catalytic reactions performed under reducing conditions, such as benzene or toluene hydrogenation and methylcyclopentane hydrogenolysis (15, 24) were in agreement with these experimental measurements as well as with theoretical calculations of the surface composition. A similar tendency was observed for reactions such as NO reduction by CO carried out under conditions close to the stoichiometry (25).

While there exists several cross-coupled techniques allowing a careful characterization of unsupported catalysts, the surface composition of small particles deposited on porous supports is not so easy to determine. In this paper, NO and CO chemisorption monitored by FTIR spectroscopy and $^{18}O_2 + {}^{16}O_2$ isotopic equilibration monitored by mass spectrometry were investigated as potential tools in characterizing the alteration of metallic surface of Pd–Rh/Al_2O_3 catalysts when fresh samples were oxidized or reduced at high temperatures (1173 K). Temperature-programmed oxidation and steam reforming of propane was also carried out over these catalysts. Because palladium is more active than rhodium in oxidation and rhodium is more active than palladium in steam reforming, the changes in activity for these reactions could be paralleled with the observations made by FTIR and isotopic equilibration.

2. EXPERIMENTAL METHODS AND PRINCIPLE OF CHARACTERIZATION

2.1. Catalysts

Because chlorine is a strong inhibitor of oxygen isotopic equilibration (OIE) (26, 27) the solids were prepared by impregnation of a γ-alumina provided by IFP (100 $m^2\ g^{-1}$) with chlorine-free precursors, $Pd(C_5H_7O_2)_2$ and $Rh(NO_3)_2$. The bimetallics were prepared by successive impregnations, Rh after Pd, with an intermediate calcination under air at 573 K. The catalysts were thus dried and calcined at 773 K under air (fresh catalysts). The total metal loading was 0.5 wt%. The solids are referred to as PdRh*x*A, where A designates alumina and *x* is the atomic percentage of Rh (Rh/Rh + Pd). The solids were aged at 1173 K under either an oxidizing (3 vol% O_2 in N_2, cooling under the mixture) or a reducing mixture (3 vol% H_2 in N_2, cooling under N_2). The treatments are referred to as "o9" (oxidizing) and "r9" (reducing), the figure "9" corresponding to the treatment temperature in hundreds of °C. For instance "PdRh25A o9" refers to the bimetallic Pd–Rh catalyst (at 25 at.% Rh) treated in 3% O_2 at 1173 K.

2.2. Chemisorption and Titration of Probe Molecules (H_2 and O_2)

H_2 chemisorption as well as O_2 and H_2 titrations were used to determine metal accessibility and total metallic area. They were carried out in a pulse chromatographic apparatus ($0.230 \pm 0.003\ cm^3$ per pulse). The catalysts (0.5 g) were reduced *in situ* in a flow of H_2 at 573 K and subsequently outgassed in Ar at 573 K and cooled down to room temperature (RT). Hydrogen chemisorption (H_C), oxygen (O_T), and hydrogen (H_T) titrations were successively recorded. Hydrogen chemisorption was shown to be partly reversible with every catalyst. H_C was determined in two steps: chemisorption at RT on the freshly reduced sample up to saturation (H_{C1}) followed by a second chemisorption on this catalyst sample outgassed for 10 min in Ar (H_{C2}). H_C was calculated by subtracting H_{C2} from H_{C1}. While O_T could be carried out at RT, Rh-containing catalysts should be heated to perform hydrogen titration, a relatively slow reaction compared to H_C and O_T. A temperature of 343 K was required to observe a ratio close to 2 between H_T and O_T. Metal accessibility (D%) was calculated using the following stoichiometries, previously verified with well-defined monometallic samples (28, 29):

$$\text{For Pd} \quad H_C : O_T : H_T = 1 : 1.5 : 3$$
$$\text{For Rh} \quad H_C : O_T : H_T = 1 : 2 : 4.$$

For the bimetallics $H_C : O_T : H_T = 1 : 1.5 + 0.5x : 3 + x$, where x is the Rh atomic fraction. Overall metallic surface area were deduced from the mean surface concentration given by Anderson (30): 21.08 μmol Pd m^{-2} and 20.75 μmol Rh m^{-2}. These values, very close for the two metals, allowed us to approximate the metal area by

$$A_m(m^2\ g^{-1}) = D\ N_T/2100,\ N_T \text{ being the total metal content in } \mu\text{mol } g^{-1}.$$

In the case of a superficial enrichment, the stoichiometry can vary, the maximum error reaching 25% for O_T. In fact, a good correlation was observed between H_T and O_T and, in this paper, the metallic surface areas have been deduced from O_T.

2.3. Oxygen Isotopic Equilibration (OIE)

The isotopic exchange was carried out in a recirculatory reactor coupled to a mass spectrometer allowing the masses 32, 34, and 36 to be monitored versus time. The home-made apparatus was described in detail elsewhere (31–33). *In situ* pretreatments were: calcination under $^{16}O_2$ at 573 K and H_2 reduction and evacuation at the same temperature. Mixtures of gaseous $^{16}O_2$ and $^{18}O_2$ containing approximately 50% of each constituent were contacted at 523 K with the solids. The analysis was performed every 9 s. The rates of equilibration were calculated on the basis of the rate of appearance of mass 34 in the gaseous phase.

The equilibration reaction, which occurs on the metal, can be written

$$^{16}O_{2\ gas} + {}^{18}O_{2\ gas} \rightarrow 2\ {}^{16}O{}^{18}O_{gas}. \qquad [1]$$

The reaction was carried out at a temperature (573 K) at which virtually no isotopic exchange with the oxygens of the solid can occur: the atomic fraction of ^{18}O in gas phase remained constant during all the experiments (typically, 1 h). It is known that OIE is very sensitive to the nature of the metal, rhodium having the highest intrinsic rate for this reaction (31, 34, 35). The sequence of the rates is Rh $\gg$ Pt $\gg$ Pd. It is therefore possible to deduce the number of Rh surface atoms. Because palladium is three to four orders of magnitude less active than rhodium, we can estimate that OIE activity is exclusively due to Rh surface atoms. The isotopic equilibration coupled with chemisorption and titrations allows the characterization of the surface state of the bimetallics. The Rh metallic surface area (A_{Rh} in $m^2\ g^{-1}$) is thus deduced from the equilibration reaction rate r_{OIE} (at.O $s^{-1}\ g^{-1}$) and the Pd metallic surface area is calculated by difference with the total metal area A_T

$$A_{Rh} = \frac{r_{OIE}}{r^*_{Rh}}, \quad [2]$$

$$A_{Pd} = A_T - A_{Rh}, \quad [3]$$

where r^*_{Rh}, the intrinsic OIE rate for Rh (at.O $s^{-1}\ m^{-2}$), was deduced from experiments carried out over monometallic Rh catalysts. The intrinsic rate of equilibration for the bimetallic catalyst is

$$r^* = \frac{r_{OIE}}{A_T}. \quad [4]$$

Combining [2] and [4] leads to the relationship

$$\frac{r^*}{r^*_{Rh}} = \frac{A_{Rh}}{A_T}. \quad [5]$$

In conclusion, knowing the total metallic area A_T (from chemisorption and titrations measurements) and the equilibration reaction rates of O_2 at 573 K, r_{OIE}, it is possible to deduce the surface composition of Pd–Rh catalysts.

2.4. FTIR Spectroscopy of Adsorbed CO and NO

For the infrared spectroscopy the samples were pressed in order to obtain thin discs of known weight (30 to 35 mg). The discs were placed in a sample holder and introduced in a cell with CaF_2 windows allowing *in situ* treatments. After reduction under H_2 at 573 K the samples were degassed at the same temperature for 60 min. After cooling to room temperature (RT) the background spectrum was recorded. Then CO or NO were admitted at 298 K under a pressure close to 10–15 Torr. The samples were also heated under 1.5 kPa NO at 473 K for 12 h. The gaseous phases were evacuated at RT in order to keep irreversibly adsorbed CO or NO. A similar procedure was previously used for characterizing Pt–Rh catalysts (36, 37). Infrared absorbance spectra were recorded at RT on a Fourier transform spectrometer (NICOLET 550) with a 4-cm^{-1} resolution. The spectra were resolved using a PEAKFIT program.

The surface composition could be deduced from FTIR using νCO and νNO bands corresponding specifically to one metallic site. In the case of reduced and oxidized monometallics, the spectra of CO adsorbed on Pd (38–43) and on Rh (36, 44–49) and of NO adsorbed on Pd (50, 51) and Rh (36, 52–56) are well known. The action of CO at 298 K induces the appearance of many bands common to both metals, but the bands assigned to the $Rh(I)(CO)_2$ species allow one to qualitatively distinguish Rh in bimetallics. The quantitative determination is ambiguous. Upon action of NO at 298 K many bands are common to both metals; so no information can be extracted from these spectra. Upon heating under NO at 473 K there is no common band since Pd gives rise to νNO bands at low wavenumbers (<1815 cm^{-1}) while a well-defined band is characteristic of Rh. In effect, on Rh/Al_2O_3, the adsorption of NO at 473 K for 12 h leads to a unique band νNO band at 1906–10 cm^{-1} assigned to $Rh(I)NO^+$ species (36, 54, 56). The conditions here used are the best conditions to obtain the oxidation of all surface Rh atoms and consequently a unique adsorption band as in references (36, 37). A linear relationship has been found between the optical density of this νNO band and the number of surface Rh atoms in Rh/Al_2O_3 samples of known dispersion. Such a relationship has been applied to Pt–Rh bimetallics by Levy *et al.* (36) and Rogemond *et al.* (37).

2.5. Transmission Electron Microscopy with X Analysis

Transmission electron microscopy in bright field mode was carried out in a Philips CM120 electron microscope operating at 120 kV with a theoretical resolution of 0.35 nm. The sample was ultrasonically suspended in ethanol and deposited on a Cu grid previously covered with a thin layer of carbon. Electron dispersive X-ray (EDX) analysis was carried out on selected area of the aged samples corresponding to metal particles of about 2 to 7 nm.

2.6. Propane Conversion in O_2 Substoichiometry

Each run was carried out at atmospheric pressure over 40 mg catalyst (diluted in 360 mg cordierite) in a dynamic reactor described elsewhere (57–60). Propane (0.4%) was injected in the reactor under substoichiometry of O_2 (0.8%) with a total flow rate of 340 $cm^3\ min^{-1}$ (reactants diluted in N_2). Direct oxidation (Eq. [6]) was limited by O_2 partial pressure, a maximal conversion of 40% being reached in C_3H_8 oxidation:

$$C_3H_8 + 5O_2 \rightarrow 4CO_2 + 4H_2O. \quad [6]$$

When O_2 is totally converted, the remaining propane may be converted into carbon oxides and H_2 (Eqs. [7], [8]) by a steam reforming reaction with the water produced in [6]

$$C_3H_8 + 3H_2O \rightarrow 3CO + 7H_2 \quad [7]$$

$$C_3H_8 + 6H_2O \rightarrow 3CO_2 + 10H_2. \quad [8]$$

For noble metal catalysts, propane oxidation is observed within the 453–623 K temperature range while propane steam reforming occurs above 623 K. In what follows, activity for propane oxidation and for propane steam reforming will be given at 573 K and at 673 K, respectively. At this latter temperature, the maximal conversion of propane by oxidation being reached, the conversion by steam reforming is calculated as the difference between the overall conversion and 40%. On the basis of Eqs. [6]–[8], a total conversion of propane cannot be reached with an inlet ratio $[O_2]/[C_3H_8]$ of 2. However, other minor reactions can occur, particularly those leading to light hydrocarbons (mainly CH_4). They make possible a 100% conversion of propane under our experimental conditions.

3. RESULTS

3.1. Overall Metallic Surface Areas

Hydrogen chemisorption gave nonreliable results for dispersion measurements: compared to titrations, excess values were sometimes obtained for the fresh catalysts while, on the contrary, much too low dispersions were recorded for sintered catalysts. This was confirmed by TEM pictures taken on representative samples. From the titrations of the H_2 and O_2 probe molecules (Tables 1 and 2), it appears that:

—there is a good accordance between dispersions deduced from both O_T and H_T whatever the catalyst treatment;

—in the case of the fresh monometallics, Pd is less dispersed than Rh on alumina. For the fresh bimetallic catalysts, the total metallic surface area (calculated per gram of metal) increases quasi linearly with the Rh content (Fig. 1). The surface composition of each bimetallic seems to be proportional to the bulk composition;

—the oxidative treatment at 1173 K induces a decrease in total metallic area, especially for the pure Rh catalyst. In fact there is formation of a nonreducible oxide phase in strong interaction with alumina, the Rh^{3+} ions diffusing into the alumina matrix (29, 61–63). Recent investigations of the structural changes of Rh/Al_2O_3 catalysts upon aging in air led to the conclusions that Rh oxides–alumina interactions could be more complex and not restricted to a mere diffusion of Rh^{3+} ions in the sublayers of alumina (64, 65). The data reported in Fig. 1 show that this phenomenon is limited in the presence of Pd. A similar cooperative effect preventing the diffusion of Rh ions in alumina was already observed in Rh–Pt bimetallic catalysts (60);

—the reducing treatment at 1173 K leads to a decrease in total metallic area, especially for Pd. The Rh catalyst is significantly less sintered than in the oxidative medium and the $Rh–Al_2O_3$ interaction is no longer observed. These results confirm that Rh/Al_2O_3 is subject to sintering only when the rhodium is in its oxide form. For the bimetallic catalysts, a quasi-linear increase of the surface area with the Rh loading is observed (Fig. 1). As for the fresh catalysts, the surface composition seems proportional to the bulk composition;

—in the case of the Pd/Al_2O_3 solid, the palladium sintering is more marked after the reducing treatment than after the oxidative one, in agreement with previous studies (8, 66, 67).

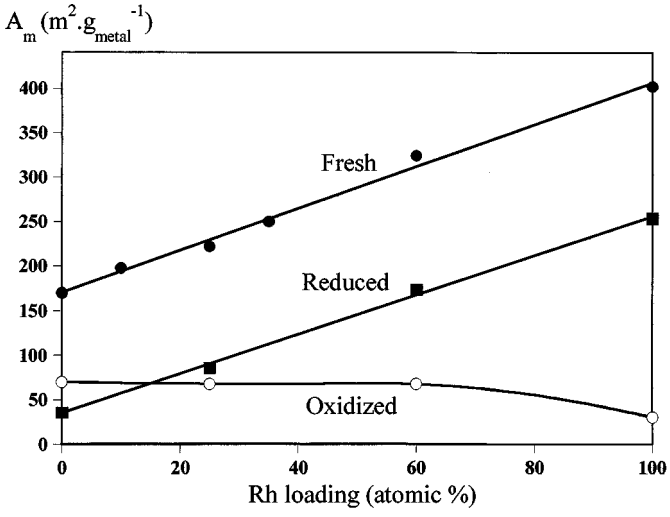

FIG. 1. Total metallic areas of fresh, reduced, and oxidized PdRh*x*A catalysts.

TABLE 1

Dispersions Deduced from O_T and H_T and Total Metallic Areas A_T (m^2/g_{solid}) of Fresh Catalysts

Solid	D (%) from O_T	D (%) from H_T	A_T (m^2/g_{solid})
PdA	38	39	0.85
PdRh10A	44	48	0.99
PdRh25A	49	53	1.11
PdRh35A	55	60	1.25
PdRh60A	71	70	1.62
RhA	87	86	2.01

3.2. Oxygen Isotopic Equilibration

For the fresh monometallic catalysts, the ratio of the intrinsic rates for Rh (1.01×10^{19} at. s^{-1} m^{-2}) and Pd (1.57×10^{15} at. s^{-1} m^{-2}) is higher than 6000. After the aging treatments, the activity per site of Rh in OIE is moderately reduced (0.75×10^{18} at. s^{-1} m^{-2} for Rh o9 and 2.08×10^{18} at. s^{-1} m^{-2} for Rh r9) while the OIE activity of Pd is practically not affected (0.74×10^{15} and 1.67×10^{15} at. s^{-1} m^{-2} for Pd o9 and Pd r9, respectively). The results obtained here with the monometallic Rh catalyst are in agreement with previous studies of Duprez and Taha (34, 68) which

TABLE 2

Dispersions Deduced from O_T and H_T and Total Metallic Areas A_T (m^2/g_{solid}) of Sintered Catalysts

	Oxidized at 1173 K (o9 samples)			Reduced at 1173 K (r9 samples)		
Solid	D (%) (O_T)	D (%) (H_T)	A_T (m^2/g_{solid})	D (%) (O_T)	D (%) (H_T)	A_T (m^2/g_{solid})
PdA	15	15	0.34	8	8	0.18
PdRh25A	11	10	0.25	19	21	0.43
PdRh60A	15	15	0.35	38	40	0.87
RhA	6	7	0.15	55	54	1.27

showed that OIE intrinsic activity was higher on small particles of rhodium than on bigger particles. However, the ratio of intrinsic rates between Rh and Pd remains high (>2500) so that the number of Rh surface atoms and the Rh surface area in the bimetallic catalysts can be deduced from their OIE rates using the monometallic as a reference. The number of Pd surface atoms and the Pd surface area are then calculated by difference with the overall number of surface atoms and the overall surface area. The results in term of surface area are given in Table 3 and are represented as a function of the atomic percentage of Rh in Fig. 2. Let us recall that the intrinsic activity ratio, in ordinates of this figure, equals the surface area ratio A_{Rh}/A_T (see Eq. [5]). From these results, it can be deduced that:

—on the fresh catalysts, there is a linear relationship between the intrinsic activity ratio and the atomic Rh content in the bimetallics. From OIE measurements, there is no detectable superficial enrichment in the fresh samples;

—the surface state of the bimetallics treated at 1173 K is strongly dependent on the nature of the mixture. The intrinsic activity ratio representing the Rh surface composition is lower than the Rh bulk composition in oxidized samples while the reverse is observed for reduced catalysts. From OIE measurements, there would be a relative increase of Pd surface area after treatment in an oxidative medium and of Rh surface area after treatment in a reducing medium.

TABLE 3

Metal Areas of Pd and Rh (m^2/g_{solid}) in Fresh and Sintered Catalysts Deduced from Oxygen Isotopic Equilibration (OIE) at 573 K

	Fresh		Oxidized at 1173 K		Reduced at 1173 K	
Catalyst	A_{Pd}	A_{Rh}	A_{Pd}	A_{Rh}	A_{Pd}	A_{Rh}
PdA	0.85	0	0.34	0	0.18	0
PdRh10A	0.87	0.12				
PdRh25A	0.89	0.22	0.25	0.003	0.27	0.16
PdRh35A	0.76	0.49				
PdRh60A	0.62	1.00	0.32	0.03	0.002	0.87
RhA	0	2.01	0	0.15	0	1.27

3.3. FTIR Spectroscopy of Fresh Monometallic Catalysts

FTIR spectra recorded over monometallic catalysts upon CO adsorption at 298 K and subsequent desorption at the same temperature are shown in Fig. 3. On initially reduced Pd/Al_2O_3 solids, it is possible to detect linear CO–Pd° species at 2062 cm^{-1} and bridged CO–Pd_2° species at 1957 cm^{-1} [(100) or (110) faces] and 1911 cm^{-1} [(111) faces]. After evacuation at 298 K, the ratio of the absorbances of the linear and bridged species reaches 0.17, in agreement with literature data (between 0.13 and 0.18) (38–43). CO adsorbed on Pd ions give rise to bands in the 2155–2150 and 2140–2110 cm^{-1} ranges (CO–Pd^{n+}). The CO adsorption at 298 K on initially reduced Rh/Al_2O_3 solids leads to linear CO–Rh° species absorbing at 2056 cm^{-1} and to bridged CO–Rh_2° species (broad absorption at around 1860 cm^{-1}) (44–48). The bands at 2097 and 2028 cm^{-1} are assigned to the symmetric and anti-symmetric νCO vibrations of the $Rh(I)(CO)_2$ gem-dicarbonyl, Rh° being partly oxidized in the presence of CO and of the OH groups of alumina (46, 47, 69) according to the reaction

$$2\,Rh + 4\,CO + 2\,AlOH \rightarrow 2\,Al\text{–}O\text{–}Rh(CO)_2 + H_2.$$

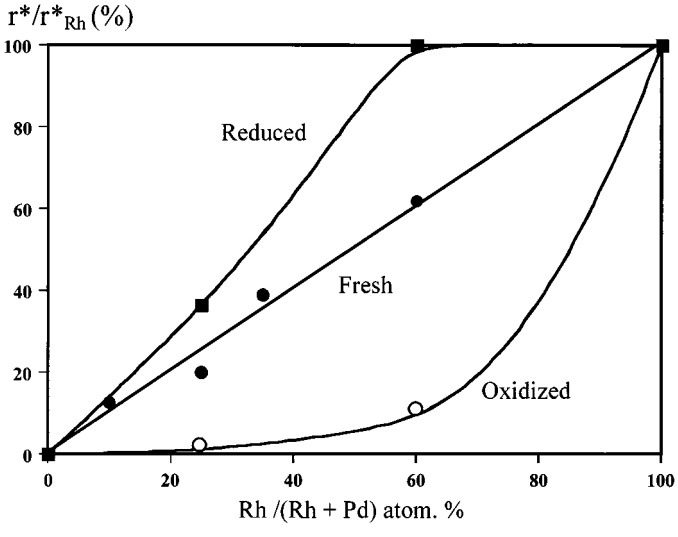

FIG. 2. Normalized intrinsic OIE rates on fresh, reduced, and oxidized PdRhxA catalysts.

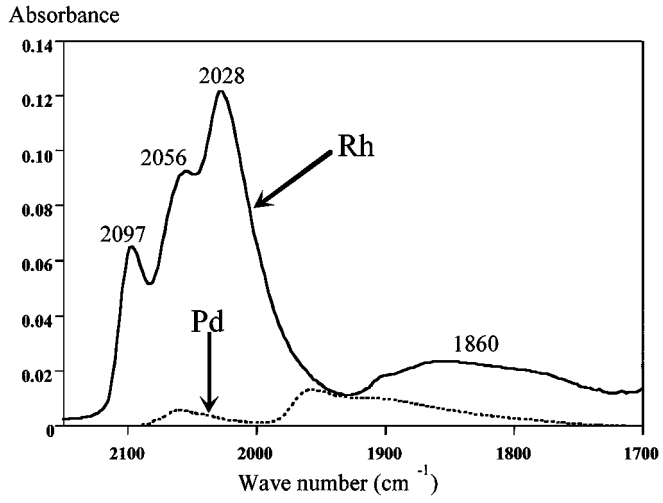

FIG. 3. Infrared spectra of CO irreversibly adsorbed at 298 K on the fresh monometallics RhA and PdA.

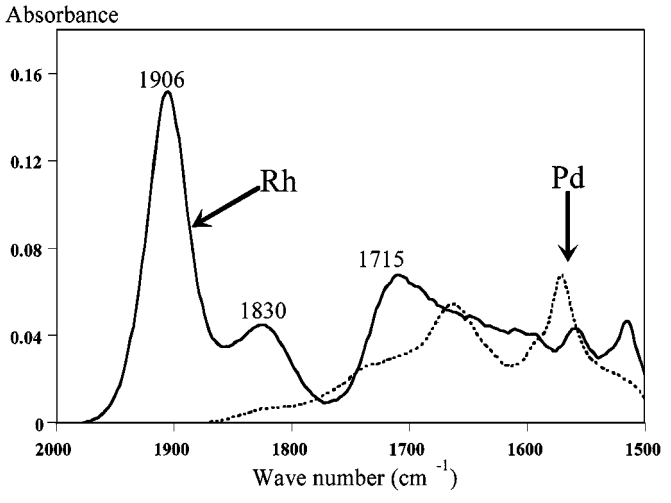

FIG. 4. Infrared spectra of NO irreversibly adsorbed at 298 K after NO treatment at 473 K of the fresh monometallics RhA and PdA.

The intensities of the bands due to CO on Rh are higher than those due to CO on Pd. For instance the absorbances of the 2028, 2097, and 2056 cm^{-1} bands reach 3.42, 2, and 2.86 per gram of Rh/Al_2O_3 solid, respectively, which corresponds to 1.7, 1, and 1.4 per m^2 Rh. The absorbance of the 1957 cm^{-1} band is equal to 0.40 per gram of Pd/Al_2O_3 solid, i.e., to 0.47 per m^2 Pd. The contribution of the Pd°–CO species, which is lower than that of $Rh(I)(CO)_2$ (ratio between 0.12 and 0.2) could be tentatively neglected in order to deduce the accessible rhodium area. The application of such a method is discussed later on in this paper.

Many bands are observed when NO is contacted with Pd° or Rh° at 298 K (spectra not shown), because of a partial oxidation of the metals. The action of NO at 298 K leads thus to the superimposition of the specific bands for Pd (50, 51) and Rh (36, 54–56). Bands of nitrates/nitrites on the support are also observed at $\nu < 1600\ cm^{-1}$ (70).

The spectra recorded after action of NO at 473K over the monometallics are shown in Fig. 4. On the Pd/Al_2O_3 solid, NO induces the appearance of bands at 1808 cm^{-1} (belonging to NO–Pd^{n+} species), at 1733 cm^{-1} (linear NO–Pd° species), at 1662 cm^{-1} (bent or bridged NO adsorbed on Pd° (50, 51), and at 1576 cm^{-1} (nitrates on the support) (70). The NO adsorption at 473 K on Rh/Al_2O_3 creates a strong band at 1906 cm^{-1} assigned to Rh(I) NO^+ species. The other bands are located at 1830 and 1715 cm^{-1} and are due to symmetric and asymmetric νNO vibrations of $Rh(NO)_2$. The 1906 cm^{-1} band is thus characteristic of superficial Rh. A calibration has been performed using the fresh (2.01 m^2 Rh/g_{solid}) and sintered (0.15 and 1.27 m^2 Rh/g_{solid}) Rh/Al_2O_3 solids. There is a linear relationship between the optical density (or absorbance) of the 1906 cm^{-1} band and the number of surface rhodium atoms (Fig. 5). The slope is equal to 2.1 with a correlation factor of 0.997. Such a correlation has already been applied to bimetallics PtRh (36, 37).

3.4. FTIR Spectroscopy of the Fresh Bimetallic PdRh25A Catalyst

On the PdRh25A bimetallic CO adsorption is performed at 298 K and NO adsorption at 473 K. Both are followed by evacuation at 298 K. For the fresh solid the action of CO induces the appearance of the bands of both metals: 2054 cm^{-1} (linear CO on Pd° and Rh°), gem-dicarbonyl $Rh(I)(CO)_2$ with two bands at 2095 and 2028 cm^{-1}, bridged species (1959 cm^{-1} for Pd°, 1883 cm^{-1} for Rh°) (Fig. 6). Neglecting the contribution of the Pd°–CO

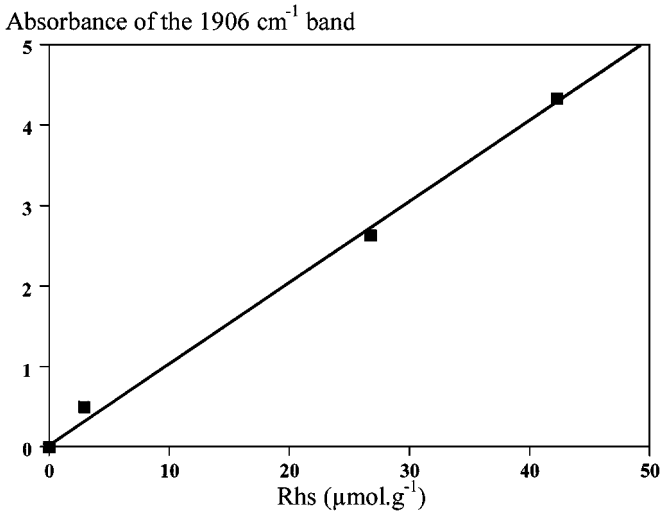

FIG. 5. Linear relationship between the optical density (absorbance) of the 1906 cm^{-1} band (per gram of solid) and the number of surface Rh atoms in monometallics Rh/Al_2O_3.

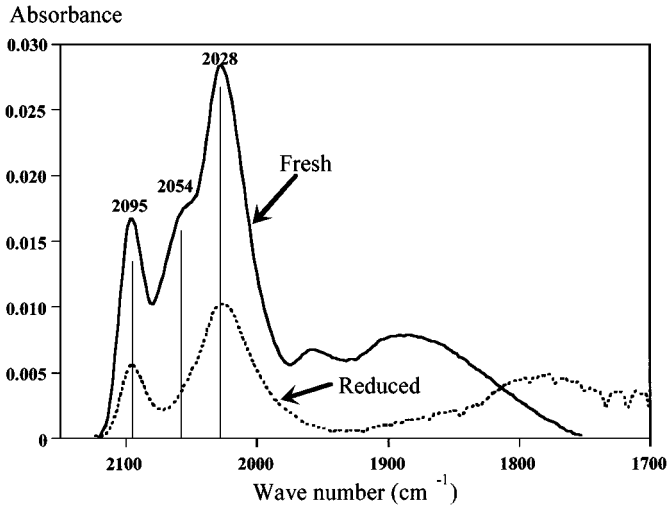

FIG. 6. Infrared spectra of CO irreversibly adsorbed at 298 K on PdRh25A, fresh and treated in reducing medium at 1173 K.

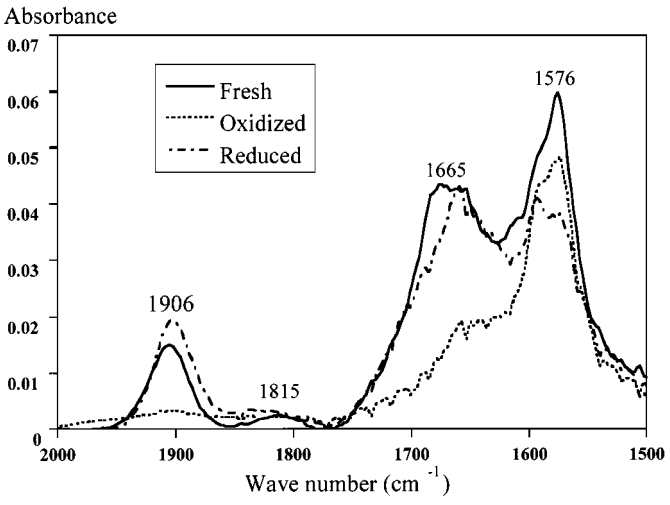

FIG. 7. Infrared spectra of NO irreversibly adsorbed at 298 K after NO treatment at 473 K of fresh and sintered PdRh25A bimetallic catalysts.

species, which is low, it could be possible to deduce the accessible rhodium provided, either the proportions of CO–Rh° and $Rh(I)(CO)_2$ species are constant, or the extinction coefficients are known, which is not the case. From resolution of the FTIR spectra, the gem dicarbonyl to linear species ratio appears to be higher in PdRh25A (3.7) than in RhA (1.8). Let us recall that this ratio increases when the rhodium particle size decreases (44–48). Because the metal dispersion is lower in the bimetallic (49%) than in RhA (87%), we can conclude that the presence of palladium promotes the formation of Rh gem-dicarbonyl species.

Upon heating under NO at 473 K (Fig. 7) there is no common band since the wavelengths due to NO on Pd are lower than 1815 cm^{-1}, and the 1906 cm^{-1} band is characteristic of Rh. From the calibration using the monometallics Rh (Fig. 5), it is possible to deduce the Rh surface in the bimetallic catalyst. The absorbance of the 1906 cm^{-1} band equals $0.45/g_{solid}$, which corresponds to 0.21 m^2 Rh/g_{solid}, in good agreement with the value deduced from the isotopic equilibration (0.22 m^2/g_{solid}) (Table 4). The presence of the 1662–1665 cm^{-1} band shows that Pd is present at the surface but the Pd surface preferably will be obtained by the difference of A_{Rh} with A_T, and not directly by infrared spectroscopy as it was already the case with OIE.

3.5. FTIR Spectroscopy of the Treated PdRh25A Solids

After treatment in oxidative medium at 1173 K, there remains practically no band due to CO irreversibly adsorbed at 298 K. In fact, from CO adsorption, Rh is no longer detected and the surface area of Pd is too weak to be quantified. After NO reaction at 473 K, the band at 1906 cm^{-1} due to Rh appears to be very weak (Fig. 7), which confirms there is almost no surface Rh atoms in PdRh25A after an oxidative treatment at 1173 K. The Rh surface area would be smaller than 0.01 m^2/g_{solid}, in good agreement with the value deduced from OEI (Table 4). The band at 1665 cm^{-1} is weak due to Pd, which indicates a decrease in Pd dispersion.

After treatment in the reducing medium at 1173 K, the spectrum of CO irreversibly adsorbed at 298 K (Fig. 6) is characteristic of Rh with bands at 2099 and 2026 cm^{-1}. Since the band at 2050 cm^{-1} appears only as a shoulder,

TABLE 4

Rhodium Surface Area of Fresh and Sintered PdRh25A Solid Deduced from OIE and FTIR after NO Treatment at 473 K and Desorption at 298 K

	Technique			
	Oxygen isotopic equilibration		FTIR of NO_{473} (band at 1906 cm^{-1})	
PdRh25A	A_{Rh} (m^2/g_{solid})	Rhodium (surf. area %)	A_{Rh} (m^2/g_{solid})	Rhodium (surf. area %)
Fresh	0.22	20%	0.21	19%
Oxidized at 1173 K	0.003	1%	<0.01	<4%
Reduced at 1173 K	0.16	37%	0.28	65%

the proportion of linear CO–Rh° species is probably weak, which would correspond to well-dispersed rhodium (45, 47, 48). The main feature is the disappearance of the 1957 and 1911 cm^{-1} bands characteristic of Pd, which could indicate a surface enrichment in Rh. From the NO reaction at 473 K (Fig. 7) and using the calibration procedure, the rhodium surface area is $0.28/g_{solid}$ (absorbance of the 1906 cm^{-1} band equal to $0.605/g_{solid}$). This value is higher than the value obtained for the fresh bimetallic ($0.21\ m^2/g_{solid}$), corroborating an enrichment into Rh, but it is higher than the value deduced from OIE ($0.16\ m^2/g_{solid}$,) (Table 4). From the infrared spectroscopy the relative increase of Rh surface area seems higher than that evidenced by OIE.

3.6. Electron Microscopy and X Analysis

Sintered catalysts were examined by electron microscopy. Even after rereduction at low temperature (573 K), the contrast between particles and support in the solid oxidized at 1173 K is very poor and does not allow one to clearly detect and analyze the metal particles. TEM pictures of the bimetallics PdRh25A treated at 1173 K in the reducing medium show particles of approximately 6 nm, which is in close agreement with the titrations results. From the EDX analysis of selected particles (about 10 particles were analyzed), the mean composition is about 95% atomic Pd and 5% atomic Rh. As both OIE and FTIR have shown that the surface is enriched into Rh, we can suppose that the particles are composed of bulk Pd with a thin layer of Rh at the surface (Fig. 8). The fraction of rhodium not analyzed by EDX would be in direct contact with the support.

3.7. Propane Conversion in O_2 Substoichiometry

The curves C_3H_8 conversion vs T(K) for the fresh catalysts are shown in Fig. 9. For the sake of comparison, the reaction profile of a standard 1% Pt/Al_2O_3 catalyst (≈50% dispersion) is also shown in the figure. The shape of these

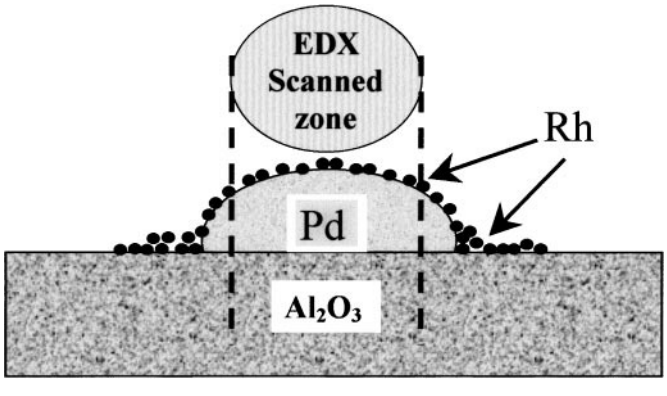

FIG. 8. Scheme of Pd–Rh particles in PdRh25A reduced at 1173 K.

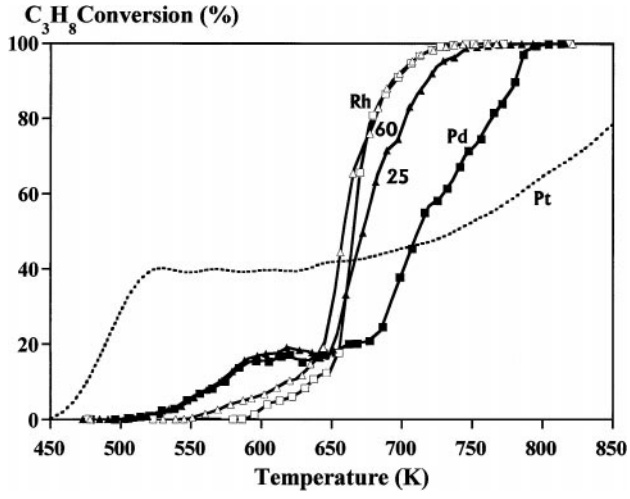

FIG. 9. Propane conversion in O_2 substoichiometry ($[O_2]/[C_3H_8] = 2$) on fresh Pd, Rh, and Pd–Rh catalysts ("60" and "25" designate the PdRh25A and PdRh60A bimetallic catalysts).

curves recorded with the monometallic catalysts has been discussed elsewhere (57–60). Let us recall that the reaction is carried out in propane excess ($O_2/C_3H_8 = 2$ instead of 5 at the stoichiometry). The oxidation reaction occurs at low temperature ($T < 620$–650 K) up to O_2 disappearance. At higher temperatures, the remaining propane is converted by steam reforming using the water produced in oxidation. The activity order for the three metals in oxidation is: Pt ≫ Pd > Rh, while the reverse order is observed in steam reforming. Only platinum can reach the maximal conversion in oxidation (40%). As Pt is not very active for steam reforming, propane conversion increases slowly above 650 K. A plateau of conversion around 20% is observed with Pd in oxidation. This was explained by a structural change of Pd (PdO → Pd°) *during* the oxidation reaction (62). As Pd° is less active than PdO for this reaction, a deactivation of the catalyst limiting the conversion at 20% is recorded. Rhodium is a poorly active catalyst for propane oxidation but it is extremely active for steam reforming. This reaction can start even before propane conversion reached 40% by oxidation. Therefore, an abrupt increase of conversion is recorded with the rhodium catalyst (Fig. 9). The curves corresponding to PdRh25A and PdRh60A are comprised between those of pure Pd and pure Rh (Pd > PdRh25A > PdRh60A > Rh in oxidation and Rh > PdRh60A > PdRh25A > Pd in steam reforming). The temperature-programmed reaction profiles of Fig. 9 allow us to calculate catalytic activity (mmol $C_3H_8\ g_{solid}^{-1}\ h^{-1}$) for oxidation at 573 K and for steam reforming at 673 K of the fresh catalysts (Table 5). Both reactions are strongly structure-sensitive and cannot be used to determine *quantitatively* metal surface area of Pd and Rh in bimetallic catalysts. For this reason, a linear relationship between activity and Rh content is not observed, PdRh25A behaving

TABLE 5

Catalytic Activity (mmol C_3H_8 g^{-1}_{solid} h^{-1}) of Fresh Pd–Rh Catalysts for Propane Oxidation at 573 K and Propane Steam Reforming at 673 K

Catalyst	Propane oxidation (573 K)	Steam reforming (673 K)
PdA	8.6	5.2
PdRh25A	8.2	14.4
PdRh60A	3.2	23.8
RhA	0.6	24.8

as pure Pd in oxidation and PdRh60A as pure Rh in steam reforming.

The specific activity of the sintered bimetallic catalysts is reported in Fig. 10. They are compared to PdAo9 and to RhAr9. PdA reduced at 1173 K shows a very low activity in oxidation while RhA oxidized at 1173 K is totally inactive for both reactions (results not shown in Fig. 10). Propane oxidation is thus a probe reaction well adapted to characterize changes in Pd surface area in oxidized catalysts while steam reforming should be chosen to evaluate Rh surface area changes in reduced samples. Normalized activity vs Rh content is shown in Fig. 11. The activity patterns confirm the results obtained by OIE and FTIR. Palladium, the active component in C_3H_8 oxidation, keeps the same activity in the oxidized bimetallics as in PdA, which suggests that the metallic phase in PdRh25A and PdRh60A should be enriched in palladium. The same behavior can be observed for Rh in steam reforming over catalysts treated at 1173 K in H_2, which indicates that reduced bimetallics are enriched in rhodium.

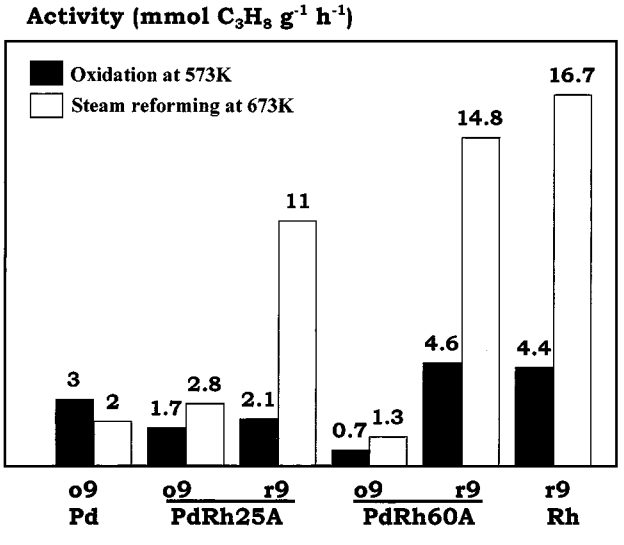

FIG. 10. Specific activity for propane conversion of Pd–Rh catalysts treated at 1173 K in 3% O_2 (o9) or in 3% H_2 (r9).

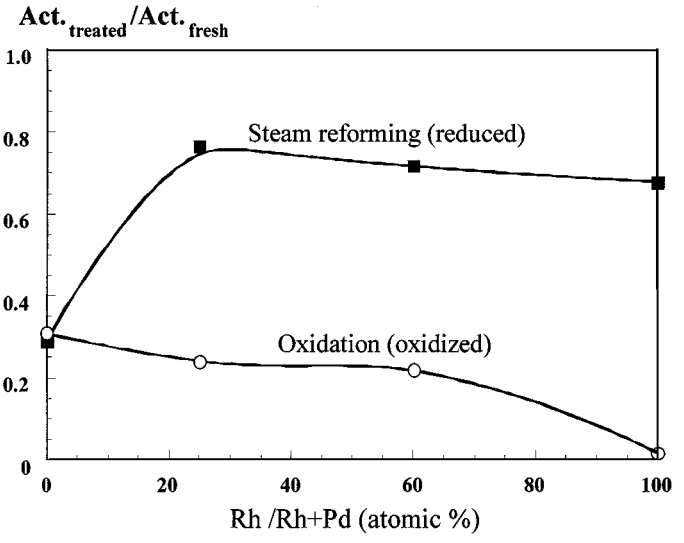

FIG. 11. Normalized activity for propane oxidation at 573 K (catalysts oxidized at 1173 K) and for propane steam reforming at 673 K (catalysts reduced at 1173 K) as a function of the Rh content in Pd–Rh catalysts.

4. DISCUSSION

4.1. Theoretical Surface Composition of Pd–Rh Particles

Two models can be used for estimating the surface composition of reduced bimetallic particles. Both models are derived from the original approach of Guggenheim for surface segregation in regular solution (71): (i) the "broken bond" model developed by Sachtler and Van Santen (72, 73) and (ii) the model developed by Wynblatt and Ku (74), very close to the regular solution model. The determining factor in the "broken bond" model is the heat of sublimation E_{sb} (also called heat of atomization): the metal having the lowest E_{sb} will segregate at the surface. The model of Wynblatt and Ku is based on differences of surface energy between the two metals: the surface would be enriched in the element having the lowest surface free energy γ_{SV} at the solid/gas interface (also called "surface tension"). For the complete determination of the surface composition, other parameters must be taken into consideration: heat of mixing and strain energy when the radius of the solute atom is larger than the radius of the solvent. However, when definite differences in γ_{SV} values are observed, there is a clear tendency to segregation. The decisive work of Tyson and Miller on the determination of surface free energy of solid metals from liquid surface tension γ_{LV} at the melting temperature T_m allowed to estimate γ_{SV} for most metals in the absence of direct experimental measurement (75). Reasonable values of the surface entropy were also estimated by Tyson and Miller to permit the calculation of γ_{SV} at any temperature below T_m. Data concerning Pd and Rh are collected in Table 6. Data concerning platinum are also given for comparison. Pd has the lowest heat of atomization and

TABLE 6

Determining Parameters of Pd and Rh for Surface Segregation in Pd–Rh Alloys: Heat of Sublimation E_{sb}, Melting Temperature T_m, and Surface Free Energy of Solid γ_{SV}

Metal	E_{sb}^a (kJ mol^{-1})	T_m^a (K)	γ_{SV} at T_m^b (J m^{-2})	γ_{SV} at 1173 K^b (J m^{-2})
Palladium	377	1825	1.743	1.874
Rhodium	557	2045	2.325	2.519
Platinum	565	2239	2.203	2.383

[a] From Ref. (76).
[b] Calculated using the method of Tyson and Miller (75).

the lowest surface free energy, which shows unambiguously that Pd should segregate at the Pd–Rh surface.

The previous models do not apply to bimetallic catalysts treated in O_2 at high temperatures since the metals are not present at the zerovalent state. The *quantitative* calculation of the surface composition appears then to be extremely complex. However, a *qualitative* tendency can be given: the bimetallic should be enriched in the metal whose oxide is the most stable. The temperatures at which the Gibbs free energy of formation of the oxides becomes nil is: Rh_2O_3 (1396 K) > PdO (1110 K) > PtO (780 K) > PtO_2 (723 K) (77). From these data, we may anticipate an enrichment in rhodium in the Pd–Rh bimetallic catalysts treated in oxidative medium. Nevertheless, the miscibility or not of the oxides, the strong interaction with the support, as is the case for rhodium oxide on alumina (61–65), might affect the primary tendency to segregation and, consequently, upset the surface composition.

4.2. Surface Composition of PdRhxA Bimetallic Catalysts

From both techniques, OIE and FTIR of NO, it is concluded that the surface composition of each bimetallics is proportional to the bulk composition as the total metallic area increases quasi-linearly with the Rh content. Using the calibration curve deduced from the adsorption of NO at 473 K on the Rh monometallics, the Rh surface calculated for the PdRh25A catalyst is in good agreement with the value deduced from the isotopic equilibration (respectively, 0.21 and 0.22 m^2/g_{solid}). Surface composition obtained by OIE on other PdRhA samples confirm the absence of any segregation effect at the bimetallic surface. At least two reasons can explain these results: (i) the bimetallics were treated at too low a temperature for activating the atomic migration process inside the metal particles, (ii) the interchange energies for this migration process ($Pd_{surf} \rightarrow Pd_{bulk}$ and $Rh_{bulk} \rightarrow Rh_{surf}$ or the reverse) become very high in the small particles present at the surface of fresh bimetallic samples.

After high temperature treatments the surface composition is strongly dependent on the nature of the gas mixture, oxidizing or reducing. In every case, we must discuss the fact that the enrichment tendency measured by OIE or FTIR was exactly the reverse of what can be calculated or anticipated by thermodynamic models (Section 4.1.).

Oxidized particles should have been enriched in rhodium. Both experimental methods detect however a decrease in surface Rh atoms. This inversion of composition is very likely due to the strong interaction between Rh ions and alumina: after the oxidative treatment the surface appears to be mostly populated with Pd atoms because of a diffusion of Rh^{3+} into the alumina matrix (61–65). A similar effect was observed with Pt–Rh/Al_2O_3 after treatment in 3% O_2 at 1173 K: while these bimetallics should have been enriched in Rh, a relative increase in Pt surface area was measured both by OIE (27) and XPS (78). Interestingly, the normal Rh enrichment was observed on the same Pt–Rh catalysts treated in oxidative medium at a moderated temperature (973 K) at which the rhodium ion diffusion in alumina occurs at a very low rate.

The treatment in the reducing medium induces a Rh surface enrichment of all the bimetallics. As in the case of the fresh bimetallics, there is a quasi linear increase of the total surface area with the Rh loading. The spectrum of CO adsorbed at 298 K on the PdRh25A solids is characteristic of rhodium. The Rh surface detected by the NO adsorption at 473 K is even higher than the Rh surface deduced from the isotopic equilibration reaction (Table 4). Activity for propane steam reforming measured over the bimetallics reduced at 1173 K (Figs. 10 and 11) confirm that these solids keep a high surface area of rhodium. Thermodynamic models anticipate the reverse situation: an enrichment in Pd in reduced alloys. The formation of a rhodium–alumina diffuse phase cannot explain the results as there is no diffusion of Rh° *into* the support. Electron microscopy coupled to EDX spectroscopy can explain this apparent discrepancy. Upon a reducing treatment at 1173 K, there is an intense sintering of the metal particles affecting more the palladium than the rhodium. The big particles are strongly enriched in Pd but the rhodium atoms form a well-dispersed phase on and *around* the metal particles (Fig. 8). The tendency of reduced rhodium to keep a relatively high dispersion on alumina (much better than reduced palladium) leads to, and explain, the conflicting results observed between theory and experimental measurements.

4.3. Hypotheses and Conditions Required for Using OIE and FTIR Methods

Both methods are based on the determination of Rh surface area in Pd–Rh bimetallics. Pd surface area is calculated by difference with the overall metallic surface area A_T. Some assumptions were made to determine A_T from O_T and H_T titrations. Because rhodium and palladium do not have the same stoichiometry of titration, A_T was initially estimated on the basis of a surface composition equal to that of the bulk. This is obviously not true for sintered

catalysts. An iterative method of correction should have been applied to calculate new A_T values and again new surface composition up to convergence of the set of values. However, we remark here that the most accurate A_T values were obtained with the fresh catalysts, which do not require a correction of the experimental values as there is no surface enrichment in these catalysts. For sintered samples, the correction will fall within the interval of error estimated to about 10% for the whole methods. In any case, these corrections cannot change the qualitative tendency observed in this study.

The isotopic equilibration allows one to measure the surface composition if there is no synergy between the metals. Furthermore the rate of isotopic equilibration is known to be structure-sensitive (34, 35). Some difficulties were encountered with Pt–Rh catalysts (27) because Rh and Pt have an opposite structure sensitivity in oxygen isotopic equilibration: intrinsic OIE rates decreased with increasing particle size of Rh while the reverse was observed with Pt. Small particles of rhodium are about two orders of magnitude more active than small particles of platinum. In contrast, big particles of Rh and Pt tend to have similar OIE rates, which require careful standardization of the data versus the particle sizes for the method to be applied. This is not the case for Pd–Rh catalysts for which the differences in OIE rates is so great that the contribution of Pd can be dropped whatever the metal dispersion. High-temperature treatments in H_2 of alumina-supported catalysts were shown to create oxygen vacancies at the periphery of metal particles. As these vacancies could be filled in by O_2 or H_2O at low temperature ($T < 500^\circ$C) (79), it is likely that the structural changes induced by these treatments in the vicinity of metal particles have no significant effects on OIE activity.

Calibrations by infrared spectroscopy have been performed on monometallics and applied to bimetallics. The νCO and νNO infrared bands are not shifted whatever the treatment; i.e., an electronic effect between Pd and Rh is not observed. We can conclude that there is no alloying effect modifying the infrared calibration coefficients. However, the adsorption could be able to modify the surface composition. For instance the gem-dicarbonyl species are formed by a chemical reaction: oxidation, during the CO adsorption, of the Rh° sites by the protons of the hydroxyls groups of the support. It is known that their proportion decreases when the rhodium particle size increases (44–49). These species prevail for highly dispersed Rh/Al_2O_3 catalysts. The study of the νCO band cannot lead to the surface Rh in bimetallics.

The characterization by FTIR spectroscopy after NO treatment at 473 K has already been discussed by Levy *et al.* (36). It is supposed that the heating under NO does not induce a migration of rhodium toward the surface for bimetallic particles. Furthermore the oxidative disruption of Rh particles under NO may modify the apparent Rh particles sizes. However, investigation of Rh/Al_2O_3 monometallic catalysts showed that the νNO vibration is not structure sensitive. Moreover, the results obtained with the bimetallic catalysts reveal that the νNO vibration is not shifted in the presence of Pd. The band at 1906 cm^{-1} may thus be regarded as a very sure way to measure Rh surface area in $Pd–Rh/Al_2O_3$ catalysts.

Finally, we have been able to relate these surface composition changes with the changes in catalytic activities, i.e., C_3H_8 oxidation and C_3H_8 steam reforming. After the oxidative treatment, the behavior is typical of palladium with a low dispersion. It is typical of rhodium after a reducing treatment (Section 3.7). Because the changes in catalytic activity are very sensitive to any modification of the surface state of the bimetallics, these results unambiguously support the measurements made by OIE and FTIR.

5. CONCLUSIONS

Oxygen isotopic equilibration (OIE) at 523 K and FTIR of CO (chemisorbed at 298 K) and NO (chemisorbed at 473 K) can be used to characterize $Pd–Rh/Al_2O_3$ bimetallic catalysts and to measure possible changes in surface composition after treatment in O_2 or H_2 at elevated temperature. However, only the rhodium surface area A_{Rh} can be measured by these techniques, which requires one to obtain the palladium surface area by subtracting A_{Rh} from A_T, the overall metal area. A_T was measured here by H_2 chemisorption and titrations (O_T and H_T). Only titrations gave reliable results. Regarding FTIR spectroscopy, the NO–Rh vibration band at 1906 cm^{-1} appears to be a very accurate method of measuring Rh surface area in Pd–Rh bimetallic catalysts.

Thermodynamic models predicting surface enrichment show that Pd–Rh alloys should be enriched in Pd under reducing conditions while a definite Rh segregation should be observed under oxidizing medium. Contrary to theory, both OIE and FTIR demonstrate that the reverse situation occurs in the series of bimetallics: enrichment in Rh in the solids treated in H_2 at 1173 K and Pd enrichment in the catalyst samples sintered in O_2 at the same temperature. These results are supported by the changes in catalytic activities for propane oxidation, a reaction for which Pd is more active than Rh, and in propane steam reforming essentially catalyzed by the rhodium.

The contradiction between theory and experimental facts can be explained by the crucial role of the support. When oxided, Rh tends to diffuse into alumina and cannot remain concentrated at the particle surface. When reduced, Rh is much more resistant to sintering than Pd and tends to be well-dispersed, but for a great part just around the metal particles. TEM and EDX carried out on a bimetallic sample reduced at 1173 K confirm that the particles are essentially composed of Pd with Rh mainly at the periphery.

Hypotheses and conditions of applications of these techniques have been discussed. The fact that the palladium surface area is determined by difference with the total area appears to be a limitation to the techniques. In the future, methods sensitive to the palladium surface area should be found to allow the surface area of each metal, Rh, and Pd to be measured independently.

REFERENCES

1. Cooper, B. J., *Plat. Met. Rev.* **38**, 2 (1994).
2. Engler, B. H., Lindner, D., Lox, E. S., Schäfer-Sindlinger, A., and Ostgathe, K., *Stud. Surf. Sci. Catal.* **96**, 441 (1995).
3. Van Yperen, R., Lindner, D., Mußmann, L., Lox, E. S., and Kreutzer, T., *Stud. Surf. Sci. Catal.* **116**, 51 (1998).
4. Kummer, J. T., *Prog. Energ. Combust. Sci.* **6**, 177 (1980).
5. Williamson, W. B., Lewis, D., Perry, J., and Gandhi, H. S., *Ind. Eng. Chem. Prod. Res. Dev.* **23**, 531 (1984).
6. Gandhi, H. S., and Shelef, M., *Appl. Catal.* **77**, 175 (1991).
7. Beck, D. D., Sommers, J. W., and DiMaggio, C. L., *Appl. Catal. B: Environmental* **3**, 205 (1994).
8. Shinjoh, H., Muraki, H., and Fujitani, Y., *Stud. Surf. Sci. Catal.* **71**, 617 (1991).
9. Williamson, W. B., Denison, G. W., Starin, G. L., and Robota, H. J., *SAE Trans.* **106**, 936 (1997).
10. Tagliaferri, S., Köppel, R. A., and Baiker, A., *Stud. Surf. Sci. Catal.* **116**, 61 (1998).
11. Chen, M., and Schmidt, L. D., *J. Catal.* **56**, 198 (1979).
12. Grill, C. M., and Gonzalez, R. D., *J. Catal.* **64**, 487 (1980).
13. Kim, S., and D'Aniello Jr, M. J., *Appl. Catal.* **56**, 23 (1989).
14. Micheaud, C., Marécot, P., Guérin, M., and Barbier, J., *Appl. Catal. A: General* **171**, 229 (1998).
15. Micheaud-Especel, C., Bazin, D., Guérin, M., Marécot, P., and Barbier, J., *React. Kin. Catal. Lett.* **69**, 209 (2000).
16. Joshi, B. M., Gandhi, H. S., and Shelef, M., *Surf. Coatings Technol.* **29**, 131 (1986).
17. Graham, G. W., Potter, T., Baird, R. J., Gandhi, H. S., and Shelef, M., *J. Vac. Sci. Technol. A* **4**, 1613 (1986).
18. Tripathi, S. N., and Bharadwaj, S. R., *J. Phase Equil.* **15**, 208 (1994).
19. Oh, S. H., and Mitchell, P. J., *Appl. Catal. B* **5**, 165 (1994).
20. Ahlström-Silversand, A. F., and Odenbrand, *Appl. Catal. A* **153**, 157 (1997).
21. Araya, P., and Diaz, V., *J. Chem. Soc. Faraday Trans.* **93**, 3887 (1997).
22. Moss, R. L., and Gibbens, H. R., *J. Catal.* **24**, 48 (1972).
23. Bertolini, J. C., Miegge, P., Hermann, P., Rousset, J. L., and Tardy, B., *Surf. Sci.* **331**, 651 (1995).
24. Del Angel, G., Coq, B., and Figueras, F., *J. Catal.* **95**, 167 (1985).
25. Holles, J. H. , Switzer, M. A., and Davis, R. J., *J. Catal.* **190**, 247 (2000).
26. Abderrahim, H., and Duprez, D., *in* "Proc. 9th Int. Cong. Catal., Calgary (1988)" (M. J. Philipps, and M. Ternan, Eds.), Vol. 3, p. 1246. The Chemical Institute of Canada, 1988.
27. Kacimi, S., and Duprez, D., *Stud. Surf. Sci. Catal.* **71**, 581 (1991).
28. Duprez, D., Pereira, P., Grand, M., and Maurel, R., *J. Catal.* **75**, 151 (1982).
29. Duprez, D., Delahay, G., Abderrahim, H., and Grimblot, J., *J. Chim. Phys.* **83**, 465 (1986).
30. Anderson, J. R., "Structure of Metallic Catalysts," p. 296. Academic Press, New York, 1975.
31. Abderrahim, H., and Duprez, D., *Stud. Surf. Sci. Catal.* **30**, 359 (1987).
32. Martin, D., and Duprez, D., *J. Phys. Chem.* **100**, 9429 (1996).
33. Holmgren, A., Duprez, D., and Andersson, B., *J. Catal.* **182**, 441 (1999).
34. Duprez, D., *Stud. Surf. Sci. Catal.* **112**, 13 (1997).
35. Descorme, C., and Duprez, D., *Appl. Catal. A: General* **202**, 231 (2000).
36. Lévy, P. J., Pitchon, V., Perrichon, V., Primet, M., Chevrier, M., and Gauthier, C., *J. Catal.* **178**, 363 (1998).
37. Rogemond, E., Essayem, N., Fréty, R., Perrichon, V., Primet, M., Chevrier, M., Gauthier, C., and Mathis, F., *J. Catal.* **186**, 414 (1999).
38. Palazov, A., Kadinov, G., Bonev, L. H., and Shopov, D., *J. Catal.* **74**, 44 (1992).
39. Duplan, J. L., and Praliaud, H., *Appl. Catal.* **67**, 325 (1991).
40. Binet, C., Jadi, A., and Lavalley, J.-C., *J. Chem. Soc. Faraday Trans.* **88**, 2079 (1992).
41. Bradshaw, A. M., and Hoffman, F., *Surf. Sci.* **72**, 513 (1978).
42. Tessier, D., Rakai, A., and Bozon-Verduraz, F., *J. Chem. Soc. Faraday Trans.* **88**, 741 (1992).
43. Gelin, P., Siedle, A. R., and Yates, J. T., *J. Phys. Chem.* **88**, 2978 (1984).
44. Yang, A. C., and Garland, C. W., *J. Phys. Chem.* **61**, 1504 (1957).
45. Primet, M., *J. Chem. Soc. Faraday Trans.* **74**, 2570 (1979).
46. Solymosi, F., and Pásztor, M., *J. Phys. Chem.* **89**, 4789 (1985).
47. Zaki, M. I., Kunzmann, G., Gates, B. C., and Knözinger, H., *J. Phys. Chem.* **91**, 1486 (1986).
48. Duprez, D., Barrault, J., and Geron, C., *Appl. Catal.* **37**, 105 (1988).
49. Trautmann, S., and Baerns, M., *J. Catal.* **150**, 335 (1994).
50. Lorimer, D., and Bell, A. T., *J. Catal.* **59**, 223 (1979).
51. Moriki, S., Inoue, Y., Miyazaki, B., and Yasumori, I., *J. Chem. Soc. Faraday Trans.* **78**, 171 (1982).
52. Solymosi, F., and Sárkány, J., *Appl. Surf. Sci.* **3**, 68 (1979).
53. Dictor, R., *J. Catal.* **109**, 89 (1988).
54. Anderson, J. A., Millar, G. I., and Rochester, C. J., *J. Chem. Soc. Faraday Trans.* **86**, 48 (1990).
55. Shelef, M., and Graham, G. W., *Catal. Rev. Sci. Eng.* **36**, 433 (1994).
56. Chafik, T., Kondarides, D. J., and Verykios, X. E., *J. Catal.* **190**, 446 (2000).
57. Maillet, T., Barbier Jr., J., and Duprez, D., *Appl. Catal. B: Environmental* **9**, 251 (1996).
58. Maillet, T., Soleau, C., Barbier Jr., J., and Duprez, D., *Appl. Catal. B: Environmental* **14**, 85 (1997).
59. Fehrat-Hamida, Z., Barbier Jr., J., Labruquére, S., and Duprez, D., *Appl. Catal. B: Environmental* **29**, 195 (2001).
60. Barbier Jr., J., and Duprez, D., *Stud. Surf. Sci. Catal.* **96**, 73 (1995).
61. Yao, H. C., Japar, S., and Shelef, M., *J. Catal.* **50**, 407 (1977).
62. Yao, H. C., Stepien, H. K., and Gandhi, H. S., *J. Catal.* **61**, 547 (1980).
63. Beck, D. D., and Carr, C. I., *J. Catal.* **144**, 296 (1993).
64. Fiedorow, R. M. J., and Wanke, S. E., *Appl. Catal. B* **14**, 249 (1997).
65. Weng-Sieh, Z., Gronsky, R., and Bell, A. T., *J. Catal.* **170**, 62 (1997).
66. Hicks, R. F., Qi, H., Young, M. L., and Lee, R. G., *J. Catal.* **122**, 279 (1990).
67. Zou, W., and Gonzalez, R. D., *Appl. Catal.* **126**, 351 (1995).
68. Taha, R., and Duprez, D., *J. Chim. Phys.* **92**, 1506 (1995).
69. Basu, P., Ponyatov, D., and Yates, J. T. Jr., *J. Amer. Chem. Soc.* **110**, 2074 (1988).
70. Ghorbel, A., and Primet, M., *J. Chim. Phys.* **73**, 1 (1976).
71. Guggenheim, E. A., *Trans. Faraday Soc.* **41**, 150 (1945).
72. Van Santen, R. H., and Sachtler, W. M. H., *J. Catal.* **33**, 202 (1974).
73. Sachtler, W. M. H., and Van Santen, R. H., *Appl. Surf. Sci.* **3**, 121 (1979).
74. Wynblatt, P., and Ku, R. C., *Surf. Sci.* **65**, 511 (1977).
75. Tyson, W. R., and Miller, W. A., *Surf. Sci.* **62**, 267 (1977).
76. "Handbook of Chemistry and Physics," 75th ed. CRC Press, Boca Raton, FL, 1994/1995.
77. Barin, I., *in* "Thermochemical Data of Pure Substances," 3rd ed. pp. 1314 and 1394. VCH, Weinheim/New York, 1995.
78. Kacimi, S., Kappenstein, C., and Duprez, D., *in* "New Frontiers in Catalysis," Proc. 10th Int. Cong. Catalysis, Budapest, 1992, Vol. 3, p. 2519. Akademiai Kiado and Elsevier, 1993.
79. Duprez, D., Sadi, F., Miloudi, A., and Percheron-Guegan, A., *Stud. Surf. Sci. Catal.* **71**, 629 (1991).